# EPR Study of γ(1,2)-$[H_nSiV^{IV}VW_{10}O_{40}]^{(7-n)-}$ ($n=0$, 1 or 2). Identification of Four One-Electron Reduction Products and Evidence for Proton Transfer in the Solid State

**Jeongmin Park and Hyunsoo So***

*Department of Chemistry, Sogang University, Seoul 121-742, Korea*
*Received April 27, 1994*

Several one-electron reduction products of γ(1,2)-$[H_nSiV_2W_{10}O_{40}]^{(6-n)-}$ were separated by precipitating or coprecipitating with diamagnetic host compounds at different pH. Mono- and diprotonated species, **1** and **2**, in powder samples exhibit EPR spectra characteristic of a mononuclear oxovanadium species, indicating that the unpaired electron is trapped at one vanadium atom. The EPR spectrum of the unprotonated species **0** shows 15 parallel lines, indicating that the unpaired electron interacts equally with two vanadium atoms. While different species were precipitated depending upon the pH of the solution and the charge of the host anion, only one species **1'** was formed in the frozen solutions at pH 3.2-4.7. The EPR spectrum of **1'** indicates that the unpaired electron is trapped at one vanadium atom and 1/16 of the spin density is delocalized onto the second vanadium atom. The species **1'** is probably another form of the monoprotonated species. The EPR spectra show that some of **2** transform into **1** and some of **0** transform into **1'** in the solid state at low temperatures. It is suggested that proton transfer between the heteropolyanion and water molecues in the solid state is involved in these transformations.

## Introduction

Mixed-valence Keggin and Dawson anions containing vanadium(IV) and vanadium(V) exhibit a variety of interesting EPR spectra. Solution spectra consisting of 15, 22, 36, and 43 lines have been observed for di- and trivanadium substituted species.[1-5] Multiline EPR spectra indicate that the unpaired electron interacts with more than one vanadium ($I=7/2$) atom, and they can be simulated by using either a hopping electron model or a delocalized electron model.[5,6] Polycrystalline EPR spectra have provided more information about the behavior of the unpaired electron in these systems. Temperature-dependent spectra indicative of intramolecular electron transfer between two vanadium atoms were observed.[7] A temperature-independent spectrum with 57 parallel lines was simulated by assuming that the unpaired electron is delocalized over three vanadium atoms, two of them being equivalent.[6]

These studies show that vanadium atom can be used as a very sensitive probe for the behavior of the unpaired electron in these metal-oxygen cluster compounds. We have extended our EPR study to reduction products of γ(1,2)-$[H_nSiV_2W_{10}O_{40}]^{(6-n)-}$, which must have the same structure as that[8] of γ(1,2)-$[PV_2W_{10}O_{40}]^{5-}$; see Figure 1. In this compound two vanadium atoms share two bridging oxygen atoms, while those in the Keggin and Dawson anions share one bridging oxygen atom. And the angle between the two V=O vectors is 31°.

## Experimental

**Preparation of Samples.** $Cs_4$ γ(1,2)-$[H_2SiV_2W_{10}O_{40}]\cdot nH_2O$ (hereafter denoted as $CsSiV_2$) was synthesized according to the literature method.[8] Its IR spectrum agrees with the reported one[8] except that the splitting of the 964 $cm^{-1}$ band is not so well resolved. As this compound was used as a coprecipitating agent, the cesium and water contents of the cesium salts precipitated at pH 4.7 and 3.7 were analyzed to determine the charge of the anion. The salt precipitated at pH 4.7. Calcd for $Cs_6[SiV_2W_{10}O_{40}]\cdot 12H_2O$: Cs 22.0, $H_2O$ 6.0. Found: Cs 22, $H_2O$ 5.84. The salt precipitated at pH 3.7. Calcd for $Cs_5[HSiV_2W_{10}O_{40}]\cdot 8H_2O$: Cs 19.4, $H_2O$ 4.22. Found: Cs 20.2, $H_2O$ 4.4.

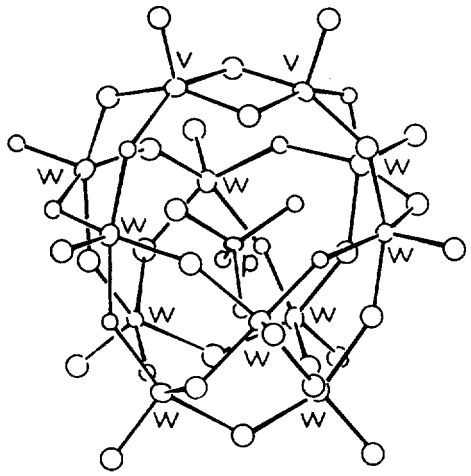


**Figure 1.** The structure of γ(1,2)-$[PV_2W_{10}O_{40}]^{5-}$. Redrawn from Figure 2 of ref 9.

$CsSiV_2$ was dissolved in a phthalate buffer of pH 3.7, and reduced by sodium dithionite. A solid (hereafter called Sample I) was precipitated by adding cesium chloride. In order to dilute Sample I in a diamagnetic host compound, Sample I and $CsSiV_2$ in the ratio of 1 : 20 were dissolved in a phthalate buffer of pH 3.7, and a solid (Sample II) was precipitated by adding CsCl.

The same procedure was followed using an acetate buffer of pH 4.7 to prepare undilute Sample III and dilute Sample IV.

The following procedure was used to prepare frozen solu-

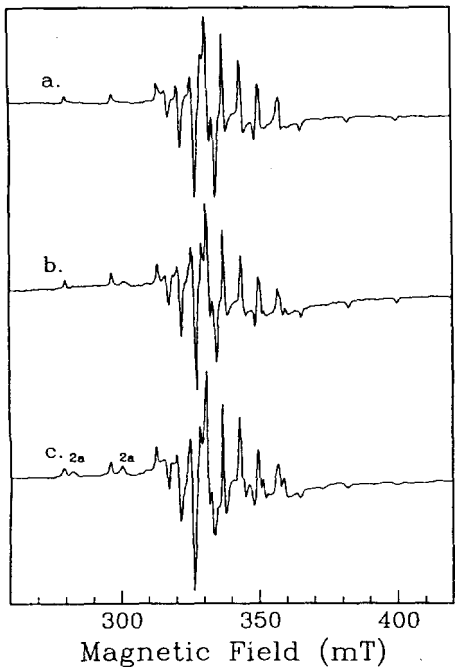


**Figure 2.** EPR spectra of (a) Sample I (undilute powder precipitated at pH 3.7) at 298 K, (b) Sample II (dilute powder precipitated at pH 3.7) at 298 K, and (c) Sample II at 77 K. In addition to the component observed at 298 K, a new component (**2a**) appears at 77 K.

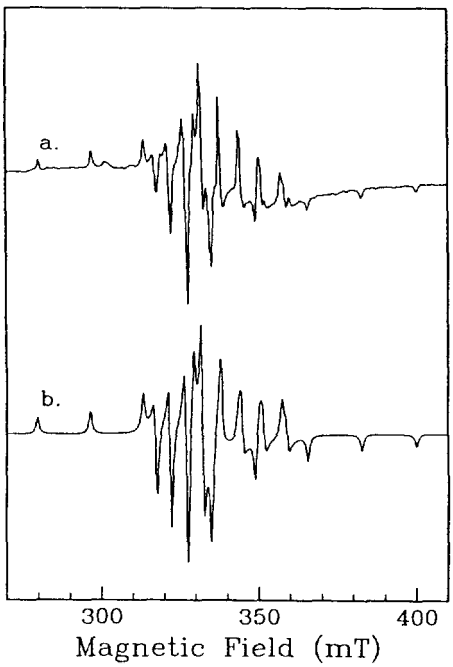


**Figure 3.** (a) Measured and (b) simulated EPR spectra of Sample II at 298 K.

tions. $CsSiV_2$ was dissolved in a buffer, reduced by adding sodium dithionite, and precipitated by adding cesium chloride. The precipitate was dissolved in the same buffer, and an equal volume of ethylene glycol was added to the solution. The mixed solution was frozen by liquid nitrogen.

**Measurements.** EPR spectra were recorded on a Bruker EPR spectrometer (Model ER 200E) operating at 9.7 GHz. The microwave frequency was measured by an Anritsu frequency counter, and DPPH was used as a g-marker. IR spectra were recorded on a Mattson FT IR spectrometer (Galaxy 2000). Cesium was determined by ICP-Mass spectrometry, and hydrated water was analyzed by TGA.

## Results and Discussion

**Diprotonated Species.** The EPR spectra of Samples I and II (undilute and dilute powder samples precipitated at pH 3.7) measured at 298 K are shown in Figures 2(a) and 2(b). Samples I and II exhibit the same spectrum (hereafter "Spectrum **2**") typical of a mononuclear oxovanadium complex. (The four chemical species reported in this paper and their EPR spectra will be designated by the number of protons attached to the heteropolyanion.) When a paramagnetic heteropolyanion is diluted into a diamagnetic host compound, the guest anion having the same charge as that of the host anion is most likely to be coprecipitated. Elemental analysis shows that the host compound precipitated at pH 3.7 is mainly $Cs_5[HSiV_2W_{10}O_{40}]\cdot 8H_2O$. Since the charge of the host anion is −5, the species **2** responsible for Spectrum **2** must be the diprotonated species, γ(1,2)-$[H_2SiV^{IV}VW_{10}O_{40}]^{5-}$.

The 77 K spectra of Samples I and II exhibit an additional component (Spectrum **2a**); the spectrum for Sample II is shown in Figure 2(c). Spectrum **2a** is attributed to a monoprotonated species; see below.

The EPR spectrum of an oxovanadium complex can be described by the spin Hamiltonian.

$$\hat{H}=\beta \boldsymbol{H}\cdot\boldsymbol{g}\cdot\boldsymbol{S}+\boldsymbol{S}\cdot\boldsymbol{A}\cdot\boldsymbol{I} \quad (1)$$

For an axial system the spin Hamiltonian may be written as

$$\hat{H}_1=\beta[g_{\parallel}H_zS_z+g_{\perp}(H_xS_x+H_yS_y)]+A_{\parallel}S_zI_z+A_{\perp}(S_xI_x+S_yI_y) \quad (2)$$

If the system responsible for Spectrum **2** is assumed to be axial, the best EPR parameters determined by simulation are $g_{\parallel}=1.9555$, $g_{\perp}=1.9670$, $A_{\parallel}=(-)0.0156$, and $A_{\perp}=(-)0.0054$ cm$^{-1}$. However, this simulation does not generate the splitting of the fourth perpendicular line into three lines, indicating that this system deviates from the axial symmetry. We have not been able to simulate the spectrum by introducing in-plane anisotropy alone. Proper simulation of the spectrum required setting the principal axes of $g$ and $A$ to be noncoincident. When the $A_3$ axis is rotated 40° from the $g_3$ axis, the observed splitting is simulated; see Figure 3. The resulting EPR parameters are $g_1=g_2=1.970$, $g_3=1.945$, $A_1=A_2=(-)0.00525$, and $A_3=(-)0.0156$ cm$^{-1}$.

**Monoprotonated Species.** Sample IV (dilute sample precipitated at pH 4.7) exhibits the same spectrum at 298 and 77 K; see Figure 4(a). Since the host compound is $Cs_6$ γ(1,2)-$[SiV_2W_{10}O_{40}]$, the guest anion must be the monoprotonated species, γ(1,2)-$[HSiV^{IV}VW_{10}O_{40}]^{6-}$. The spectrum (Spectrum **1**), which is similar to that of a mononuclear oxovanadium complex, could be simulated nicely using the axial spin Hamiltonian given in Eq. (2); see Figure 4(b). The resulting EPR parameters are $g_{\parallel}=1.914$, $g_{\perp}=1.964$, $A_{\parallel}=(-)$

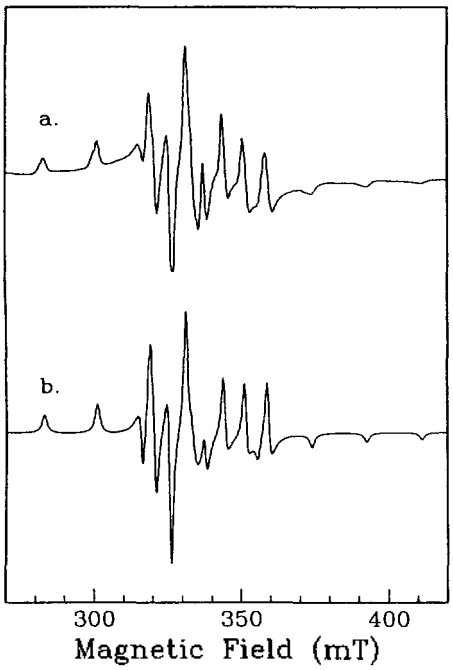


**Figure 4.** (a) Measured and (b) simulated EPR spectra of Sample IV (dilute powder precipitated at pH 4.7). The spectra measured at 298 and 77 K are the same.

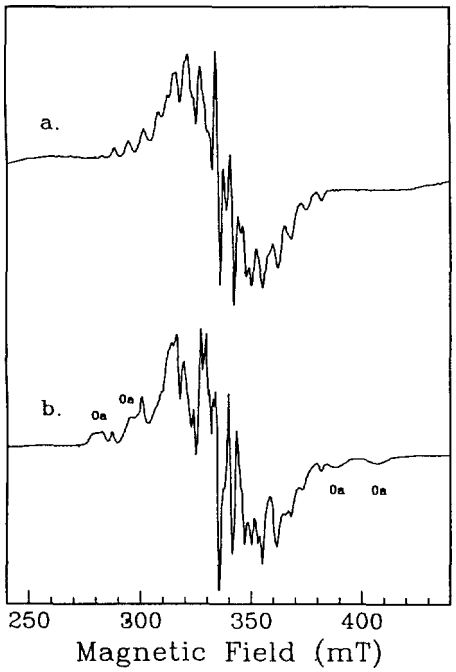


**Figure 5.** EPR spectra of Sample III (undilute powder precipitated at pH 4.7) measured at (a) 298 and (b) 77 K. The broad component observed at room temperature disappears and a new component (**0a**) appears at 77 K.

0.0164, and $A_{\perp}=(-)0.00563$ cm$^{-1}$.

On close examination of Spectrum **1** we note that each of the broad parallel lines consists of several lines. This suggests that several closely related species contribute to Spectrum **1**. A sample prepared by controlled potential electrolysis exhibited two such species.

**Unprotonated Species.** The EPR spectra of Sample III (undilute sample precipitated at pH 4.7) measured at 298 and 77 K are shown in Figure 5. The 298 K spectrum consists of a broad component and a component (Spectrum **0**) having 15 "parallel" lines. At 77 K the broad component disappears and a new component (Spectrum **0a**) appears. Since the species **0** responsible for Spectrum **0** is not coprecipitated with $Cs_6$ $\gamma$(1,2)-$[SiV_2W_{10}O_{40}]$ at pH 4.7, it must be the unprotonated species, $\gamma$(1,2)-$[SiV^{IV}VW_{10}O_{40}]^{7-}$. The broad component may be attributed to a two-electron reduction product. Spectrum **0a** appearing at low temperature agrees with the frozen solution spectrum; see below.

Spectrum **0** is similar to that of $\alpha$(1,2)-$[PV^{IV}VW_{10}O_{40}]^{6-}$, in which the unpaired electron interacts with two equivalent vanadium atoms.[3,6] Some hyperfine lines seem to be broadened at 77 K, indicating that the electron transfer rate is temperature-dependent. When an electron is hopping between two sites, modified Bloch equations can be used to describe the EPR line shape.[5,6] This method has been used successfully to simulate the solution EPR spectra of various mixed-valence compounds. We have extended this method to the simulation of Spectrum **0** which is a polycrystalline spectrum. Our approach is to calculate the positions of eight hyperfine lines expected when the unpaired electron is trapped at each vanadium atom for a given direction of the magnetic field, then to calculate the spectrum for each combination of two nuclear spin states using modified Bloch equations, and finally to add up the spectra for all possible combinations of the nuclear spin states and for all possible directions of the magnetic field.

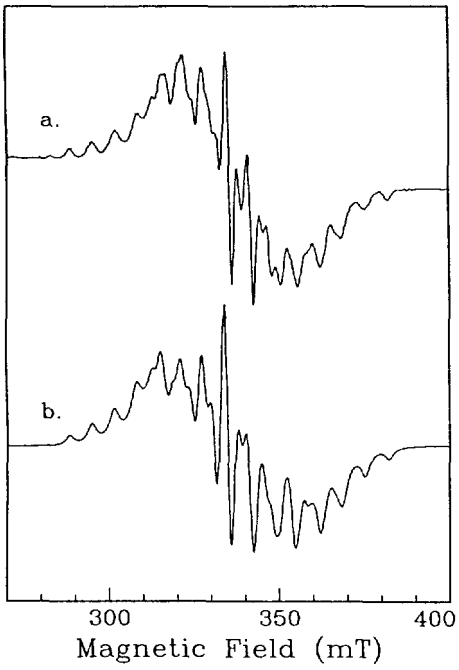


**Figure 6.** (a) Measured and (b) simulated EPR spectra of Sample III at 298 K.

In order to simulate Spectrum **0** we assume that the principal axes of $g$ and $A$ coincide, the $g_3$ axes are parallel to the V=O vectors, and the $g_1$ axes lie in the plane containing

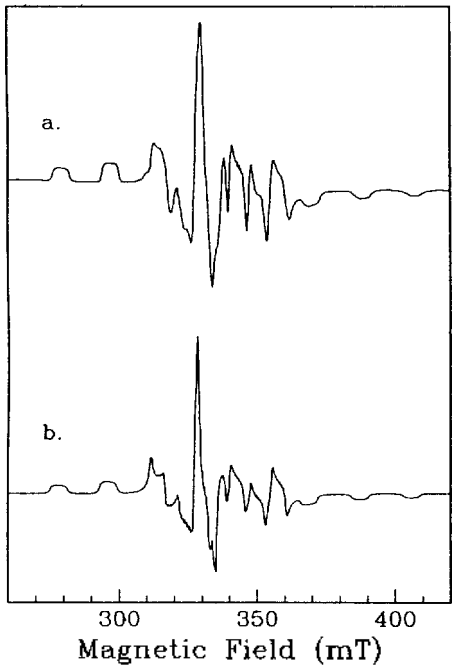


**Figure 7.** (a) Measured and (b) simulated frozen solution EPR spectra of Sample I or III.

two V=O vectors. A simulated spectrum is shown in Figure 6(b). The parameters used for simulation are $g_1=1.947$, $g_2=1.975$, $g_3=1.984$, $A_1=A_2=(-)0.0060$, $A_3=(-)0.0128$ $cm^{-1}$, and $P=2.6\times10^{10}$ $s^{-1}$. Here $P$ is the transition probability per second for the intramolecular electron transfer. Although most of the observed lines are accounted for, the intensity distribution of the inner lines is not simulated satisfactorily. The discrepancy may originate in the assumption that the principal axes of $g$ and $A$ are coincident. The imperfect simulation makes it difficult to determine an accurate transition probability.

The broad component, which is indicative of a strong dipolar interaction, may be assigned to a two-electron reduction product. The relative intensity of this component depended upon the amount of reducing agent added. The fact that its intensity decreases as the temperature is lowered shows that it originates in the excited triplet state, the ground state being a singlet. Such excited state EPR spectrum was observed for the copper(II) acetate dimer.[11] The two-electron reduction product can also explain the sharpness of the EPR spectrum observed for Sample III. If Sample III were a pure one-electron reduction product, its spectrum would be quite broad because of the intermolecular dipolar interaction. As the species **0** was diluted in the two-electron reduction product, it exhibited a sharp spectrum. A broad component showing a similar behavior was also observed for Sample I.

**Frozen Solution Spectrum.** The same EPR spectrum was observed for the frozen solutions at pH 3.2, 3.7 and 4.7. This spectrum (Spectrum **1'**) shown in Figure 7(a) is different from any spectrum attributed to un-, mono-, or diprotonated species above. Its parallel lines have flat tops, and one perpendicular line exhibits superhyperfine structure with a splitting of 0.67 mT. The spectrum can be simulated by

**Table 1.** EPR Parameters of γ(1,2)-$[H_nSiV^{IV}VW_{10}O_{40}]^{(7-n)-}$ Species

| | **2** | **1** | **0** | **1'** |
|---|---|---|---|---|
| $g_1$, $g_2$ ($g_\perp$) | 1.970 | 1.964 | 1.947, 1.975 | 1.969 |
| $g_3$ ($g_\parallel$) | 1.945 | 1.914 | 1.984 | 1.940 |
| $A_1$, $A_2$ ($A_\perp$) | −52.5 | −56.3 | −60.0 | −57.0 |
| $A_3$ ($A_\parallel$) | −156.0 | −164.0 | −127.5 | −165.0 |
| $B_1$, $B_2$ | | | | −5.4 |
| $B_3$ | | | | −7.4 |

*Hyperfine coupling constants are in units of $10^{-4}$ $cm^{-1}$. Their signs are assumed to be negative.

assuming that the unpaired electron is trapped at one vanadium atom with partial delocalization onto the other vanadium atom. The appropriate spin Hamiltonian is as follows:

$$\hat{H}=\hat{H}_1+B_1S_{x2}I_{x2}+B_2S_{y2}I_{y2}+B_3S_{z2}I_{z2} \quad (3)$$

The $z_2$ axis was assumed to lie along the second V=O vector which cants away from the first V=O vector by 31°. The simulated spectrum is shown in Figure 7(b). The resulting parameters are $g_\parallel=1.940$, $g_\perp=1.969$, $A_\parallel=(-)0.0165$, $A_\perp=(-)0.0057$, $B_1=B_2=(-)0.00054$, and $B_3=(-)0.00074$ $cm^{-1}$. The isotropic hyperfine coupling constants for two vanadium atoms are 0.0093 and 0.00061 $cm^{-1}$. If the isotropic hyperfine coupling constant is used as a measure of the unpaired electron density on the vanadium atom, the ratio of the unpaired electron density on two vanadium atoms is 15 : 1.

The species **1'** responsible for Spectrum **1'** is the only species trapped in the frozen solution at pH 3.2-4.7. It is also formed from **0** in the solid state at low temperatures. Probably a proton transfer is involved in this transformation; see below. The species **1'** has most of the unpaired electron density at one vanadium atom and only 1/16 of it at the second vanadium atom. If the extent of delocalization of the unpaired electron onto the second vanadium atom is compared, **1'** lies between the diprotonated species for which the unpaired electron is trapped at one vanadium atom and the unprotonated species for which the electron interacts equally with two vanadium atoms. These results lead us to believe that **1'** is another monoprotonated species. We have already seen a monoprotonated species **1** which does not exhibit any superhyperfine structure. Thus **1'** and **1** should have different configurations. It is intriguing that the monoprotonated species can have different configurations in the matrix of a host compound and in the frozen solution.

It is remarkable that only **1'** is trapped in the frozen solutions at pH 3.2-4.7. This means that all other one-electron reduction species, which have been in equilibrium with **1'** in solution, transform into **1'** in the process of freezing.

**EPR Parameters.** The EPR parameters of the four species are listed in Table 1. The parameters of **1** and **1'** are similar to those of other heteropolyanions containing one oxovanadium ion.[12,13] Although the parameters of **2** are normal, the principal axes of $g$ and $A$ are noncoincident. EPR spectra of most oxovanadium complexes could be intepreted in terms of an axial spin Hamiltonian. For an axial system, the principal axes of $g$ and $A$ are coincident, and one of them

is parallel to the V=O vector. But **2** shows a feature characteristic of a severe noncoincidence of the principal axes of $g$ and $A$. A similar noncoincidence was found for an oxomolybdenum compound, $[MoO(SCN)_5]^{2-}$, for which the $A_3$ axis deviates slightly from the Mo=O axis, but the $g_3$ axis is rotated 14° from the Mo=O vector.[14] While the orientation of the $A$ matrix is determined primarily by that of the nonbonding $d_{xy}$ orbital, the principal axes of the $g$ matrix are determined by the orientations of the orbitals of the excited states which are mixed into the ground state *via* spin-orbit coupling. So the principal axes of $g$ and $A$ need not coincide, but the rotation of the $g_3$ axis by 40° from the $A_3$ axis is difficult to explain.

The parameters of **0** look peculiar, for $g_3$ is larger than the other g values. Such reversal has never been observed for oxovanadium complexes. The small $A_3$ value is similar to that of $[HPV^{IV}V_2W_9O_{40}]^{6-}$, in which the unpaired electron trapped at one vanadium atom is partially delocalized onto the other two vanadium atoms.[7]

**Proton Transfer in the Solid State.** Now that the EPR spectra of un-, mono-, and diprotonated species have been identified, the spectral components appearing at 77 K may be assigned. Spectrum **2a** in Figure 2(c) agrees with Spectrum **1**. This means that some of the diprotonated species **2** transform into the monoprotonated species **1** by proton transfer from **2** to a hydrated water molecule at low temperature. Temperature dependence of the spectrum indicates that the proton transfer is reversible for fresh samples.[15]

Spectrum **0a** in Figure 4(b) coincides with Spectrum **1'**, indicating that some of the unprotonated species **0** transform into the monoprotonated species **1'**. The source of the proton is probably not the hydrated water molecules, for **0** cannot be more basic than $OH^-$. Then the proton must come from an oxonium ion which is in the vicinity of the heteropolyanion in the crystal. X-ray structural analysis has revealed that crystals of some heteropoly compounds contain oxonium ions.[16]

These results suggest the following scheme for the transformation of the species.

$$H_2SiV^{IV}V\ (\mathbf{2}) \underset{+H^+}{\overset{-H^+}{\rightleftharpoons}} HSiV^{IV}V\ (\mathbf{1}) \uparrow\downarrow HSiV^{IV}V\ (\mathbf{1'}) \underset{+H^+}{\overset{-H^+}{\rightleftharpoons}} SiV^{IV}V\ (\mathbf{0})$$

Although transformation between **1** and **1'** has not been observed directly, formation of **1'** only in the frozen solutions at pH 3.2-4.7 suggests such transformation.[17]

Solid-state thermal isomerizations of some heteropolyanions were reported,[18,19] but their energetics are poorly understood. Proton transfer in the solid state containing heteropolyanions has not been reported so far. As was pointed out by Finke *et al.*,[19] solid-state rearrangements of polyanions may be more general and proton transfer may induce such rearrangements in some cases.

**Effect of Protonation on Molecular Structure.** We will assume that $\gamma(1,2)$-$[SiV^{V}VW_{10}O_{40}]^{7-}$ has essentially the same structure as $\gamma(1,2)$-$[PV_2W_{10}O_{40}]^{5-}$ shown in Figure 1. The vanadium atoms are connected by two bridging oxygen atoms. The V-O-V angle (97°) shows that the contribution of the oxygen 2*s* orbital to the V-O bonding is relatively small. The unpaired electron in the $V^{4+}$ ion resides in the $3d_{xy}$ orbital, and overlap of two $3d_{xy}$ orbitals provides the pathway of electron transfer between the two vanadium atoms. For the unprotonated species, the extent of this overlap is large enough to allow the unpaired electron to interact equally with the two vanadium nuclei.

Now we consider the protonated species. Terminal and bridging oxygen atoms are potential sites for protonation. The protonation behavior of polyvanadates and vanadotungstates suggested that the bridging oxygen atoms are more basic than the terminal oxygen atoms.[20-22] There are several types of bridging oxygen atoms in $\gamma(1,2)$-$[SiV^{IV}VW_{10}O_{40}]^{7-}$: those between two tungsten atoms, those between one tungsten atom and one vanadium atom, and those between two vanadium atoms. When a hexavalent tungsten atom in a heteropolyanion is replaced by a pentavalent vanadium atom, the bridging oxygen atoms bonded to the vanadium atom get extra negative charges.[23] So the oxygen atoms between two vanadium atoms are most basic, and they must be protonated preferentially.

When the bridging oxygen atom $O_b$ is protonated, the V-$O_b$ bond length is expected to increase. X-ray structural analyses of polyvanadates have revealed that protonation of $O_b$ increases the V-$O_b$ bond distance by 0.05-0.10 Å[20,24]. In addition, the V-$O_b$-V angle is expected to increase on protonation, for $sp^3$ hybrid orbitals of $O_b$ are involved in the V-$O_b$ bonding. The V-$O_b$-V angles in a hexavanadate fall in the range 109-113°, indicating that $sp^3$ hybrid orbitals are used in the V-$O_b$ bonding even when the oxygen atom is unprotonated.[24] In this case protonation of $O_b$ causes no significant change in the V-$O_b$-V angle. However, when the V-$O_b$-V angle is 97°, it may increase by *ca* 10° on protonation. These changes cause considerable lengthening of the V···V distance. Model building shows that the angle between two V=O vectors also increases on protonation to accomodate the elongated $V_2O_8$ moiety in the heteropolyanion framework. All these changes decrease overlap of the two $3d_{xy}$ orbitals. This explains why the electron is trapped at one vanadium atom for the diprotonated species.

Now the intermediate case is the monoprotonated species. Actually two different species have been identified. The species **1** is coprecipitated at pH 4.7 with $Cs_6$ $\gamma(1,2)$-$[SiV_2W_{10}O_{40}]$, and formed from the diprotonated species **2** in the solid state at low temperature. So the structure of **1** seems to be closely related to that of **2**. On the other hand, **1'** is trapped in the frozen solution at pH 3.2-4.7, and formed from the unprotonated species **0** in the solid state at low temperature. So **1'** seems to be closely related structurally with **0**.

The existence of two monoprotonated species may be explained in terms of the V-$O_b$-V angle. When $O_b$ is protonated, the V-$O_b$(H)-V angle is *ca* 109° because of the $sp^3$ hybrid orbitals involved. When $O_b$ is not protonated, the V-$O_b$-V angle can be either *ca* 109° ($sp^3$) or *ca* 90° ($p^3$). Therefore, when a proton is removed from **2**, the V-$O_b$-V angle need not change from *ca* 109°. This monoprotonated species, which will have essentially the same structure as **2**, may be **1**. On the other hand, when a proton is added to **0**, one of the V-$O_b$-V angles should change from 97° to *ca* 109°. This monoprotonated species, which has a large V-$O_b$(H)-V angle and a small V-$O_b$-V angle, may be **1'**. Since any change in the V-$O_b$-V angle is associated with a considerable adjust-

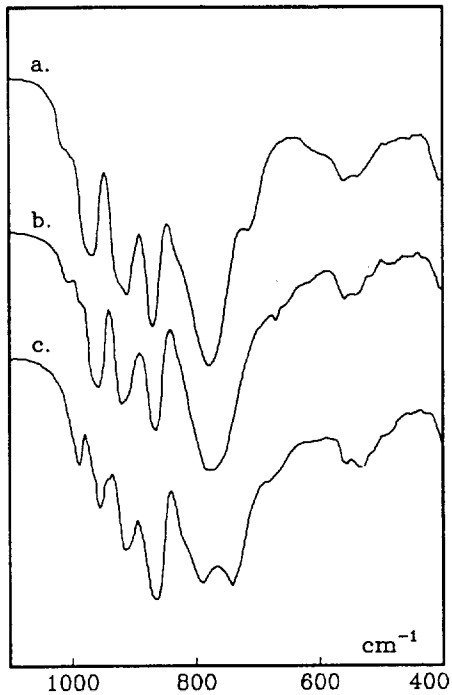


**Figure 8.** Infrared spectra of (a) $Cs_4$ γ(1,2)-$[H_2SiV_2W_{10}O_{40}]\cdot nH_2O$, (b) $Cs_5$ γ(1,2)-$[HSiV_2W_{10}O_{40}]\cdot nH_2O$, and (c) $Cs_6$ γ(1,2)-$[SiV_2W_{10}O_{40}]\cdot nH_2O$.

ment in the whole framework of the anion, an energy barrier can exist between these two monoprotonated species.

The effect of protonation on the molecular structure is also reflected in the IR spectra of $Cs_{6-n}$ γ(1,2)-$[H_nSiV_2W_{10}O_{40}]$ ($n=2$, 1 or 0); see Figure 8. The IR spectrum of the diprotonated species exhibit four prominent bands at 700-1100 $cm^{-1}$ similar to those of the α-$[SiW_{12}O_{40}]^{4-}$, for which the bands were assigned to the stretchings of the following groups: 967-981 (W=O), 920-928 (Si-O), and 878-894 and 780-797 $cm^{-1}$ (W-$O_b$-W, W-$O_c$-W).[25,26] Here $O_b$ and $O_c$ represent the bridging oxygen atom between corner-sharing octahedra, and that between edge-sharing octahedra, respectively. γ(1,2)-$[H_2SiV_2W_{10}O_{40}]^{4-}$ is expected to exhibit similar bands in addition to the bands characteristic of the γ structure and the $V_2O_8$ moiety. Some additional bands appear overlapped with the bands at 964 and 909 $cm^{-1}$. In fact, the 964 $cm^{-1}$ band is split into two lines in the IR spectrum reported previously.[8] One of these lines may originate in the stretching of V=O.

The effect of deprotonation is clearly seen in the spectra. The band at 866 $cm^{-1}$ and the bands at 909-918 $cm^{-1}$ undergo no significant change on deprotonation. The band at 777 $cm^{-1}$ band is broadened for the monoptonated species, and split into two bands at 741 and 791 $cm^{-1}$ for the unprotonated species. The 964 $cm^{-1}$ band shifts to lower frequency as the proton is removed, and an additional band appears at 988 $cm^{-1}$ for the unprotonated species. However, it is difficult to explain these changes in terms of the degree of protonation.

**Concluding Remarks.** We have detected at least four different one-electron reduction products of γ(1,2)-$[H_nSiV_2W_{10}O_{40}]^{(6-n)-}$ by EPR spectroscopy. Temperature-dependent transformations between some species in the solid state suggest that proton transfer is involved. The EPR spectra have provided considerable information on the structures of these species. However, several unsolved problems remain: (1) Why is the $g_3$ axis rotated 40° from the $A_3$ axis in **2**? (2) What causes the proton transfer in the solid states? In addition, a complete simulation of Spectrum **0** is also an unsolved problem. More work is needed, including EPR study of dilute single crystals, to clarify these problems.

**Acknowledgment.** Financial support from the Korea Science and Engineering Foundation is gratefully acknowledged.

## References

1. Mossoba, M. M.; O'Connor, C. J.; Pope, M. T.; Sinn, E.; Hervé, G.; Tézé, A. *J. Am. Chem. Soc.* **1980**, *102*, 6864.
2. Harmalker, S. P.; Leparulo, M. A.; Pope, M. T. *J. Am. Chem. Soc.* **1983**, *105*, 4286.
3. Lee, C. W.; So, H. *Bull. Korean Chem. Soc.* **1986**, *7*, 39.
4. Lee, C. W.; So, H.; Lee, K. R. *Bull. Korean Chem. Soc.* **1986**, *7*, 108.
5. So, H.; Lee, C. W.; Lee, D. *Bull. Korean Chem. Soc.* **1987**, *8*, 384.
6. Lee, C. W.; So, H. *Bull. Korean Chem. Soc.* **1986**, *7*, 318.
7. So, H.; Lee, C. W. *Bull. Korean Chem. Soc.* **1990**, *11*, 115.
8. Canny, J.; Thouvenot, R.; Tézé, A.; Hervé, G.; Leparulo-Loftus, M.; Pope, M. T. *Inorg. Chem.* **1991**, *30*, 976.
9. Domaille P. J.; Harlow, R. L. *J. Am. Chem. Soc.* **1986**, *108*, 2108.
10. Lee, C. W.; So, H.; Lee, K. R. *Bull. Korean Chem. Soc.* **1988**, *9*, 362.
11. Bleaney, B.; Bowers, K. D. *Proc. Roy. Soc.* **1952**, *A214*, 451.
12. So, H.; Flynn, Jr., C. M.; Pope, M. T. *J. Inorg. Nucl. Chem.* **1974**, *36*, 329. The parameters for $[VW_5O_{19}]^{4-}$ are $g_{\parallel}=1.949$, $g_{\perp}=1.969$, $A_{\parallel}=(-)0.0167$, and $A_{\perp}=(-)0.0061$ $cm^{-1}$.
13. Smith, D. P.; So, H.; Bender, J.; Pope, M. T. *Inorg. Chem.* **1973**, *12*, 685. The parameters for $[PVW_{11}O_{40}]^{5-}$ are $g_{\parallel}=1.910$, $g_{\perp}=1.966$, $A_{\parallel}=(-)0.0167$, and $A_{\perp}=(-)0.00593$ $cm^{-1}$.
14. Nilges, M. J.; Belford, R. L. *J. Magn. Resonance* **1979**, *35*, 259.
15. It was found that some species had been transformed irreversibly into oher species one year after preparation.
16. Knoth, W. H.; Domaille, P. J.; Harlow, R. L. *Inorg. Chem.* **1986**, *25*, 1577.
17. It was found that **2** had been transformed into **1** one year after preparation. Some of **1** thus formed is transformed reversibly into **1'** at low temperatures.
18. Knoth, W. H.; Domaille, P. J.; Farlee, R. D. *Organometallics* **1985**, *4*, 6268.
19. Finke, R. G.; Droege, M. W.; Domaille, P. J. *Inorg. Chem.* **1987**, *26*, 3886.
20. Day, V. W.; Klemperer, W. G.; Maltbie, D. J. *J. Am. Chem. Soc.* **1987**, *109*, 2991.
21. Flynn, Jr., C. M.; Pope, M. T. *Inorg. Chem.* **1971**, *10*, 4091.
22. Finke, R. G.; Rapko, B.; Saxton, R. J.; Domaille, P. J. *J. Am. Chem. Soc.* **1986**, *108*, 2947.
23. Day, V. W.; Klemperer, W. G. *Science* **1985**, *228*, 533.
24. Chen, Q.; Goshorn, D. P.; Scholes, C. P.; Tan, X.; Zubieta,

J. *J. Am. Chem. Soc.* **1992**, *114*, 4667.
25. Lange, G.; Hahn, H.; Dehnicke, K. Z. *Naturforschg.* **1969**, *24b*, 1498.
26. Rocchiccioli-Deltcheff, C.; Fournier, M.; Franck, R.; Thouvenot, R. *Inorg. Chem.* **1983**, *22*, 207.

# Synthesis of Aminophosphonopeptides Containing Carbapenem

**Ik Joong Kang*, Kyu Wan Lee†, Wan Joo Kim†, and Yong Joon Kim**

*Department of Chemical Engineering, Kyungwon University, Sungnam 461-701, Korea*
*†Korea Research Institute of Chemical Technology, Taejon 305-606, Korea*
*Department of Chemical Engineering, Korea University, Seoul 136-701, Korea*
*Received May 6, 1994*

A new kind of aminophosphonopeptides containing carbapenem, allyl-(5*R*,6*S*)-3-(2-carbobenzyloxyamino-3-dialkylphosphonopropionyl-2-amino)ethanthio-6-{(1′*R*)-hydroxyethyl}-7-oxo-1-azabicyclo[3.2.0]hept-2-ene-carboxylate **1a-1d**, have been synthesized. 2-Carbobenzyloxyamino-3-dialkylphosphonopropionyl-2-amino-ethanethiol **7a-7d**, aminophosphonopeptides, were produced starting from *N*-carbobenzyloxyserine methyl ester (**2**) and 2-amino-3-dialkyl-phosphonopropionate (**4**) by way of methyl 2-carbobenzyloxyamino-3-dialkylphosphonopropionate **5a-5d**. The coupling of amino-phosphonopeptides **7a-7d** and allyl (5*R*,6*S*)-6-{(1′*R*)-hydroxyethyl}-1-aza-3,7-dioxobicyclo[3.2.0]-heptane-2-carboxylate yielded aminophosphonopeptides containing carbapenem **1a-1d**.

## Introduction

Since 2-aminoethylphosphonic acid (2-AEPn) was isolated from sheep rumen in 1959 by Horiguchi and his coworkers,[1] many aminophosphonic acids and their derivatives have been discovered in living organism. Aminophosphonic acids are also discovered in mammalian tissues such as human muscle, sheep liver, and bovine brain.[2-8] Its concentration in human tissues was higher in heart and skeletal muscle than in liver and brain. It has been known that the compounds having carbon-phosphorus bond are also stable. Aminophosphonic acids and their derivatives have attracted attenion because of their antibiotic, herbicidal, pesticidal, anticancer, and enzyme inhibitory activities and because of particulary their structural similarities to biologically important amino acids.

Recently, incorporated with synthetic derivatives, biological activity of aminophosphonopeptides were widely investigated. Kleinrok *et al.*[9] investigated central pharmacological properties of aminophosphonic acids and their derivatives. Among various disciplines neurochemistry and neuropharmacology are the most brisk areas concerning the activity of aminophosphonic acid. The effect of ω-phosphono-α-aminocarboxylic acid on seizures and brain level in E1 mice was tested.[10] Carbapenem has a different structure from penicillin and cephalosporin and has a broader antibiotic, antibacterial activity and resistance to hydrolysis by β-lactamase. There were many carbapenem derivatives containing amide-bonded alkylthiol group at C-3 position which were synthesized because of their antibiotic activity.[11-19] Atherton[20] reported phosphonopeptides containing penicillin or cephalosphorin synergisted antibiotic activity. Phosphonopeptides are structurally divided into two groups, one containing carbon-nitrogen bond and the other amide containing phosphorus-nitrogen bond. Phosphonopeptides containing C-N amide bond was found to be a strong competitive inhibitor of peptide hydrolysis enzyme. Jacobson[21] reported *N*-[[[(benzyloxycarbonyl)amino]methyl]hydroxyphosphonyl]-L-phenylalanylalanine was an active inhibitor of carboxypeptidase A. Elliott[22] also observed that phosphonopeptides containing C-N amide bond was an effective inhibitor of enkephalinase in kidney of rat and brain of man. Phosphonopeptides containing P-N amide bond have antibiotic activity because they inhibit biosynthesis of peptidoglycan in bacterial cellwall as well as penicillin and cephalosphorin antibiotics. Allen[23] synthesized alaphosphorin which is a dipeptide of 1-aminoethylphosphonic acid and L-alanine and showed its antibacterial and antiviral activities. Niida[24] and Bayer[25] separated bialafos(phosphinothricylalanylalanine) from a fermentation broth of *Streptomyces hygroscopicus* and *Stretomyces viridochromogens*, and discovered its broad antibiotic activity for Gram positive and Gram negative bacteria.

Now we accomplished a total synthesis of new aminophosphonopeptides containing carbapenem **1a-d**. In this paper, the authors wish to report the synthesis of allyl-(5*R*,6*S*)-3-(2-carbobenzyloxyamino-3-dialkylphosphonopropionyl-2-amino)ethanethio-6-{(1′*R*)-hydroxyethyl}-7-oxo-1-azabicyclo[3.2.0]hept-2-ene-carboxylate **1a-d**, as shown in Scheme 1.

## Results and Discussion

A synthesis of allyl (5*R*,6*S*)-(2-carbobenzyloxyamino-3-dialkylphosphonopropionyl-2-amino)ethanthio-6-{(1′*R*)-hydroxyethyl}-7-oxo-1-azabicyclo[3.2.0]hept-2-ene-carboxylate **1a-d** was carried out using inexpensive chemicals. *N*-carbobenzyloxyserine methyl ester (**2**) was tosylated to give *O*-tosyl *N*-carbobenzyloxyserine (**3**)-in 86% yield. Methyl 2-carbobenzyloxyamino-3-dialkylphosphonopropionate (**5**) was prepared in